Dexterous Force Estimation during Finger Flexion and Extension Using Motor Unit Discharge Information

Yang Zheng and Xiaogang Hu

Abstract— **With the development of advanced robotic hands, a reliable neural-machine interface is essential to take full advantage of the functional dexterity of the robots. In this preliminary study, we developed a novel method to estimate isometric forces of individual fingers continuously and concurrently during dexterous finger flexion and extension. Specifically, motor unit (MU) discharge activity was extracted from the surface high-density electromyogram (EMG) signals recorded from the finger extensors and flexors, respectively. The MU information was separated into different groups to be associated with the flexion or extension of individual fingers and was then used to predict individual finger forces during multi-finger flexion and extension tasks. Compared with the conventional EMG amplitude-based method, our method can obtain a better force estimation performance (a higher correlation and a smaller estimation error between the predicted and the measured force) when a linear regression model was used. Further exploration of our method can potentially provide a robust neural-machine interface for intuitive control of robotic hands.**

I. INTRODUCTION

Recently, a variety of advanced robotic hands have been developed with the ability to control individual fingers [1-3], which makes it possible for individuals with arm amputation or hand impairment to perform dexterous finger movements for rehabilitative or assistant purposes. In order to take full advantage of these robots, a reliable neural-machine interface is needed to transfer human movement intention into robot control command. Among different kinds of neural signals [4-6] to predict finger kinematics, surface electromyogram (EMG) signals have the advantage of non-invasive nature, low cost, high signal-to-noise ratio, and stable data recordings, and therefore show promising application prospects [7, 8].

Pattern recognition techniques have been widely used to decode the movement intention from EMG recordings [9]. Typically, EMG signals during different hand motions were captured and the global features were extracted for individual motions. Then, the features were fed into a classifier to classify between different motions. In this way, some specific motions can be recognized and translated into the predefined commands. Although a large number of hand motions can be recognized with an accuracy as high as 96% [9], the pattern recognition-based method cannot decode the motions in a continuous manner and therefore, the robot hand cannot be controlled continuously. Instead, proportional control [10, 11] can be used to control a specific degree of freedom in a continuous manner. Global features such as the EMG amplitude were extracted continuously and used as the control input of robots. However, due to some factors that can substantially affect the EMG recordings, such as the background noise, motion artifacts, and the cancellation of superimposed motor unit action potentials (MUAP), the control performance can decrease significantly. In order to address these issues, previous studies have demonstrated that the motor unit (MU) discharge information decoded from the EMG signals [12, 13] was less affected by these factors, and can be a more robust measurement of the muscle activation level when fingers performed isometric extension [14-16]. However, only finger extension was involved, and EMG signals were captured from the extensor digitorum communis (EDC) muscle that is superficial to the skin surface. It is not clear whether the MU discharge information can be extracted accurately from the deeper flexor digitorum superficialis (FDS) muscle to predict the finger flexion force. In addition, it needs to be investigated how to predict dexterous finger force when both flexion and extension are involved.

Accordingly, we utilized the MU discharge information to predict force output when fingers performed dexterous isometric flexion and extension (i.e. individual fingers flexed and extended sequentially or concurrently). High-density EMG (HD-EMG) recordings were recorded from the EDC and FDS muscles. MU discharge information was extracted, and the neural drive signal was estimated from the populational MU discharge frequency of the EDC and FDS, respectively for individual fingers. The neural drive signals were then used to predict the finger flexion or extension force with a linear regression model (termed neural-drive method). The conventional force prediction method using the EMG amplitude (root mean square) information was also performed as a comparison (EMG-amp method). The results showed that the neural-drive method can obtain a better force prediction performance compared with the EMG-amp method when a linear regression model was used. A further exploration of the proposed method can potentially provide a robust neural-machine interface for intuitive control of advanced robotic hands with manual dexterity.

II. METHODS

A. Subjects

Three neurologically intact subjects were recruited in this study. All subjects gave informed consent with protocols approved by the Institutional Review Board of the University of North Carolina at Chapel Hill.

B. Experimental Setup

During the experiment, the forearm of the subjects was supported with a foam in a neutral position and the wrist was restrained from movements using two stiff foam pads. The

index, middle, ring and pinky fingers were secured to four load cells (SM-200N, Interface), respectively to measure the finger flexion and extension force with a sampling rate of 1000 Hz (Figure 1). The real-time force data was displayed on a monitor with the target force level.

Two 8×16 HD-EMG electrode arrays covered the posterior and anterior sides of the forearm to measure EMG activities from the EDC and FDS, respectively (Figure 1). The individual electrodes have a 3-mm diameter with a 10-mm inter-electrode distance. Using the EMG-USB2+ system (OT Bioelettronica), monopolar EMG signals were amplified and sampled at 2048 Hz with the reference placed at the wrist. The amplifier was set to have a gain of 1000 and a pass band of 10–900 Hz.
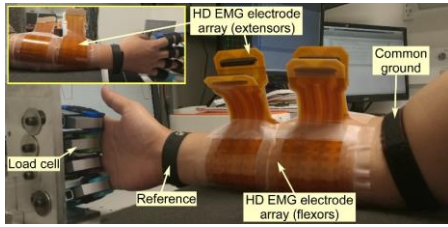

Figure 1: Experimental setup. Two 8×16 HD-EMG electrode arrays measuring the EMG activities from the extensor digitorum communis and the flexor digitorum superficialis, respectively, and four load cells measuring individual finger flexion and extension forces.

C. Experimental Procedures

Since two motion types (finger flexion and finger extension) were involved in this study, the maximum voluntary contraction (MVC) forces of isometric flexion and extension were first measured separately for individual fingers. Due to the enslaving effect between the ring and pinky fingers, the subjects were requested to extend or flex the two fingers concurrently, and their forces were summed up. Predefined force traces required subjects to follow a repeated trapezoidal pattern that had a maximum flexion and extension force of 50% of their finger-specific flexion and extension MVC, respectively. Two different types of trials were performed. In the first type, the subjects were asked to flex or extend one specific finger (index, middle, or ring-pinky) in a trial, while avoiding co-contractions of other fingers (single-finger trial). For each finger, four trials for flexion and extension were performed resulting in a total of eight single-finger trials. In the second type, two or three fingers flexed and extended in sequence within a trial (multi-finger trial), and co-contraction of other fingers was allowed. The order of fingers in the multi-finger trials was random, and 16 multi-finger trials were performed in total.

D. Data Analysis

EMG signals were first filtered using a high-pass filter at 10 Hz and the motion artifacts were removed using an independent component analysis-based algorithm [17].

1) Force prediction using the neural-drive method

The neural-drive method to predict finger force includes four steps, i.e., EMG decomposition, MU pool refinement, neural drive estimation, and force prediction.

EMG decomposition. The separation vector $\mathbf{w}$ of individual MUs was first obtained by decomposing the EMG signals from the single-finger trials using the Fast-ICA

algorithm [18] that has been used in our previous studies [14, 15]. If the task of a single-finger trial was finger flexion/extension, then only the EMG from the corresponding muscle was used to extract the MU information. The source signal $\mathbf{s}$ can be obtained by multiplying the separation vector with the extended and whitened EMG signal $\mathbf{Z}$:

$$\mathbf{s} = \mathbf{wZ} \qquad (1)$$

The MU discharge activity i.e., spike train $\mathbf{T}$, was obtained by classifying the peaks of the source signal using the *Kmeans++* algorithm.

Figure 2A illustrates the force data of a representative trial with middle finger extension. The spike trains of the MUs obtained from the same trial are illustrated in Figure 2B. Based on the finger (index, middle, or ring-pinky) and the motion type (flexion or extension), the MUs decomposed from individual trials were initially pooled into 6 MU groups for the extension and flexion of individual fingers, respectively.
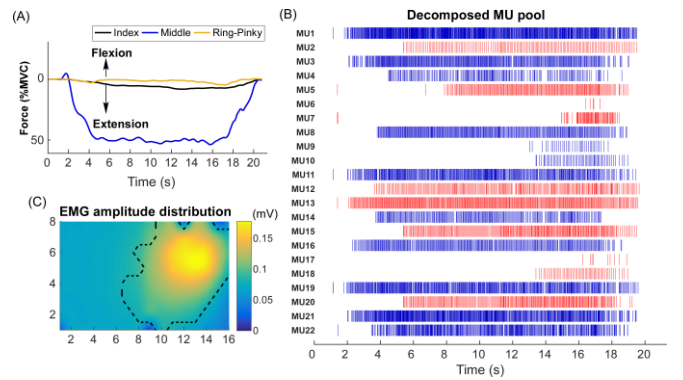

Figure 2: The force data of a representative single-finger trial with middle finger extension (A). The spike trains of individual MUs decomposed using the EMG signal from finger extensors of the trial (B). The MUs with red spike trains were excluded from the MU pool of the middle finger extension after the refinement procedure. The EMG amplitude (root mean square) distribution from finger extensors of the trial (C). The dashed lines encircled the channels used in the EMG-amp method.

MU pool refinement. A refinement procedure was used to remove the MUs that were falsely identified into a specific group. The MUs obtained from a single-finger trial of a specific finger might be associated with the muscle of other fingers because muscle contraction of other fingers still existed to some degree. Multi-finger trials were used to refine the MU pool. Since the multi-finger trials were also used to evaluate the force prediction performance (see below), the multi-finger trials were randomly divided into four groups, and a four-fold cross evaluation was performed to avoid in-sample optimization, which has been used previously [19, 20]. The MU pool refinement was performed using the training set while the prediction performance was evaluated using the testing set.

Specifically, for a given multi-finger trial, the separation vector of a MU from a specific finger (for example, middle finger) and motion type (for example, extension) was applied to the corresponding EMG signal using Equation (1), resulting in a source signal and a spike train [14]. Then, the firing rate was calculated from the spike train using a 0.5-second-long sliding window with a step of 0.1 second (all sliding windows are the same in the subsequent text unless otherwise noted). A linear regression analysis was performed between the firing

rate and the force signals of individual fingers, obtaining three coefficient of determination values (R^2) corresponding to three fingers. This procedure was repeated for all multi-finger trials in the training set, and the three R^2 values were averaged across all trials. If the R^2 of the specific finger (middle) was larger than that of other fingers (index and ring-pinky), the MU was kept in the MU pool. Otherwise, the MU was excluded. The rational was that the firing rate of the MUs was associated with the force level. The red spike trains illustrated in Figure 2B were removed from the MU pool for the middle finger extension and the blue ones were retained. To this end, the MUs in a pool were considered to solely reflect the flexion or extension of a specific finger.

Neural drive estimation. For a given multi-finger trial, the separation vectors of individual MU pools were applied to the EMG signals using Equation (1) to obtain the spike trains of individual MUs. The firing rate of individual MUs was calculated using the sliding window and summed up across all MUs for individual MU pools. The firing rate summation represented the neural drive signal for individual MU pools.

Force prediction. After obtaining the neural drive signal of individual MU pools, a two-variable linear regression analysis between the force data and the two (extension and flexion) neural drive signals was performed for individual fingers:

$$F = a \cdot D_{extensor} + b \cdot D_{flexor} \qquad (2)$$

where F was the force, $D_{extensor}$ and D_{flexor} were the neural drive of extension and flexion, respectively. The resultant R^2 value and root mean square error (RMSE) between the actual force and predicted force were averaged across all trials from the testing set to evaluate the force prediction performance.

2) Force prediction using the EMG-amp method

The performance of the neural-drive method was compared with the conventional EMG-amp method. The EMG channels used for individual fingers were also selected via a two-step procedure. The first step used the single-finger trials to select the top 60 channels that had the maximum EMG amplitude when individual fingers moved. When the motion type of a single-finger trial was finger flexion or extension, only the corresponding EMG signals were considered. After the first step, the EMG channels were divided into 6 groups with each representing a specific finger and a motion type. This preliminary EMG channel classification procedure can lead to substantial overlap of channels between fingers. Therefore, the second step was performed to refine the EMG channel groups for individual fingers and motion types using the multi-finger trials in the training set. For a given multi-finger trial, the EMG amplitude of individual channels of all groups was calculated using the sliding window and a linear regression analysis was performed between the EMG amplitude and the force of individual fingers, resulting in three R^2 values for each EMG channel. For a given EMG channel group of a specific finger, if a channel had a larger R^2 value with the specific finger compared with the other two fingers, then the channel was kept. Otherwise, the channel was removed. Figure 2C shows the EMG amplitude distribution from finger extensors of a single-finger trial with the middle finger extension and the dashed lines encircled the channels for the middle finger extension after the EMG channel refinement procedure. The procedure was repeated across all

groups until all groups were refined. The force prediction procedure of the EMG-amp method was similar with the neural-drive method. Instead of calculating the neural drive signal of individual pools, the EMG amplitude was averaged across all retained channels for individual groups.

III. RESULTS

Figures 3A and B illustrate the spike trains of individual MUs for the index extensor and the flexor, respectively, from a representative multi-finger trial in the testing set. The thick curves in Figure 3A and B represent the normalized neural drive signal calculated as the firing rate summation across all MUs in the pool. Figure 3C illustrates the force prediction results of individual fingers using both the neural-drive method and the EMG-amp method from the same trial. The neural-drive method can predict the force accurately in most cases. On the contrary, the force predicted using the EMG-amp method had both overestimation and underestimation issues, especially for the index finger. In some cases, the EMG-amp method can even predict the force to the opposite direction, such as the force of the middle and ring-pinky fingers at around 3 second with the extension force falsely estimated as the flexion force.
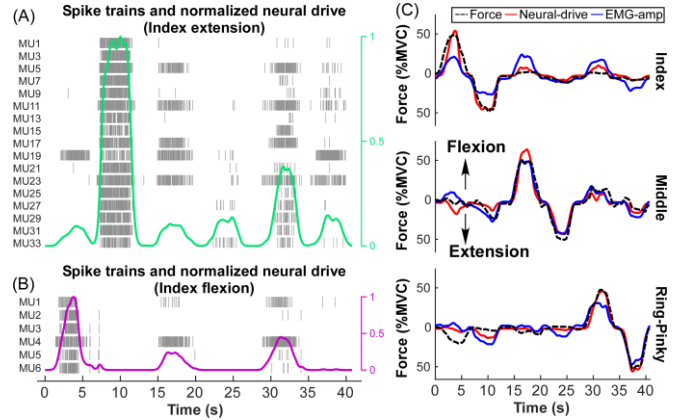

Figure 3: The spike trains and neural drive signals of the index extension (A) and flexion (B), respectively of a representative multi-finger trial. Only odd-numbered MUs are illustrated to save space for the extension. The corresponding force prediction results of the trial (C).

The average R^2 values and RMSE across the four-fold cross-evaluation are shown in Table I for individual subjects. The results showed that for all subjects, the R^2 value using the neural-drive method was larger than that of the EMG-amp method. In addition, the RMSE using the neural-drive method was smaller than that of the EMG-amp method for all subjects.

TABLE I.   FORCE PREDICTION PERFORMANCE

Sub.	R^2		RMSE (%MVC)	
	Neural-drive	EMG-amp	Neural-drive	EMG-amp
1	0.765	0.666	8.657	10.471
2	0.821	0.752	5.953	7.811
3	0.666	0.561	8.063	10.108

IV. DISCUSSION

In this study, a novel method was developed to predict isometric finger flexion and extension forces based on the discharge information of MUs. Our preliminary results demonstrated that by extracting the MU discharge information from the finger flexors and extensors separately, the

neural-drive method can predict the isometric finger force accurately when the fingers performed dexterous flexion and extension. In addition, the neural-drive method had a better force prediction compared with the conventional EMG-amp method when a linear regression model was used, manifested as a higher correlation and a lower estimation error.

Compared with the EMG-amp method, the neural-drive method had less overestimation and underestimation problems. For the EMG-amp method, the overestimation and underestimation issue was mainly from the cross-talk of EMG activities between different fingers due to proximity of finger muscle compartments [21]. Even though an EMG channel refinement procedure was performed to exclude the overlap of channels between different fingers, it is still possible for an electrode to capture the EMG activities of different fingers. On the contrary, the neural-drive method was less affected by the crosstalk activities, which demonstrated the potential of the neural-drive method to distinguish the muscle activation between anatomically close muscles. The overestimation and underestimation in the neural-drive method mainly came from the false positive or negative firing events because the separation matrix used to extract firing events was obtained using different EMG data. Some other factors might also influence the performance of the EMG-amp method, but may had less influence on the estimation of the neural drive signal, such as background noise and motion artifacts [17].

The MU number identified from the extensors was larger than that from the flexors (Figure 3A and B). The possible reason was that the position of the FDS muscle is deeper than that of the EDC muscle. The proximity to the skin surface leads to a larger amplitude and a narrower width of the MUAP and therefore more identified MUs.

One limitation of the current study was that only a simple two-variate linear regression model was used to establish the relation between the force and the information (neural drive or EMG amplitude) of extensors and flexors. However, since the force output can be affected by the contraction of both extensors and flexors. The linear regression model might be insufficient to explain the complex condition when antagonists contract concurrently. In our future study, more complex models will be tested to evaluate whether the force prediction performance can be further improved. In addition, more subjects will be recruited and more metrics such as the time delay will be used to verify the performance of the neural drive method in predicting dexterous finger flexion and extension forces.

REFERENCES

[1] B. N. Perry, C. W. Moran, R. S. Armiger, P. F. Pasquina, J. W. Vandersea, and J. W. Tsao, "Initial clinical evaluation of the modular prosthetic limb," *Frontiers in neurology,* vol. 9, pp. 153, 2018.

[2] H. In, B. B. Kang, M. Sin, and K.-J. Cho, "Exo-glove: A wearable robot for the hand with a soft tendon routing system," *IEEE Robotics & Automation Magazine,* vol. 22, no. 1, pp. 97-105, 2015.

[3] O. Van Der Niet Otr, H. A. Reinders-Messelink, R. M. Bongers, H. Bouwsema, and C. K. Van Der Sluis, "The i-LIMB hand and the DMC plus hand compared: a case report," *Prosthetics and orthotics international,* vol. 34, no. 2, pp. 216-220, 2010.

[4] S. Gribi, S. d. B. de Dunilac, D. Ghezzi, and S. P. Lacour, "A microfabricated nerve-on-a-chip platform for rapid assessment of

[5] T. A. Kuiken, G. Li, B. A. Lock, R. D. Lipschutz, L. A. Miller, K. A. Stubblefield, and K. B. Englehart, "Targeted muscle reinnervation for real-time myoelectric control of multifunction artificial arms," *Jama,* vol. 301, no. 6, pp. 619-628, 2009.

[6] G. Santhanam, S. I. Ryu, M. Y. Byron, A. Afshar, and K. V. Shenoy, "A high-performance brain–computer interface," *nature,* vol. 442, no. 7099, pp. 195, 2006.

[7] N. Nazmi, M. Abdul Rahman, S.-I. Yamamoto, S. Ahmad, H. Zamzuri, and S. Mazlan, "A review of classification techniques of EMG signals during isotonic and isometric contractions," *Sensors,* vol. 16, no. 8, pp. 1304, 2016.

[8] A. Fougner, Ø. Stavdahl, P. J. Kyberd, Y. G. Losier, and P. A. Parker, "Control of upper limb prostheses: terminology and proportional myoelectric control—a review," *IEEE Transactions on neural systems and rehabilitation engineering,* vol. 20, no. 5, pp. 663-677, 2012.

[9] A. A. Adewuyi, L. J. Hargrove, and T. A. Kuiken, "An analysis of intrinsic and extrinsic hand muscle EMG for improved pattern recognition control," *IEEE Transactions on Neural Systems and Rehabilitation Engineering,* vol. 24, no. 4, pp. 485-494, 2015.

[10] K. Z. Zhuang, N. Sommer, V. Mendez, S. Aryan, E. Formento, E. D'Anna, F. Artoni, F. Petrini, G. Granata, and G. Cannaviello, "Shared human–robot proportional control of a dexterous myoelectric prosthesis," *Nature Machine Intelligence,* vol. 1, no. 9, pp. 400-411, 2019.

[11] J. G. Ngeo, T. Tamei, and T. Shibata, "Continuous and simultaneous estimation of finger kinematics using inputs from an EMG-to-muscle activation model," *Journal of neuroengineering and rehabilitation,* vol. 11, no. 1, pp. 122, 2014.

[12] C. Dai, and X. Hu, "Independent component analysis based algorithms for high-density electromyogram decomposition: Experimental evaluation of upper extremity muscles," *Computers in Biology and Medicine,* vol. 108, pp. 42-48, 2019.

[13] F. Negro, S. Muceli, A. M. Castronovo, A. Holobar, and D. Farina, "Multi-channel intramuscular and surface EMG decomposition by convolutive blind source separation," *Journal of neural engineering,* vol. 13, no. 2, pp. 026027, 2016.

[14] Y. Zheng, and X. Hu, "Real-time isometric finger extension force estimation based on motor unit discharge information," *Journal of neural engineering,* vol. 16, no. 6, pp. 066006, 2019.

[15] C. Dai, Y. Cao, and X. Hu, "Prediction of individual finger forces based on decoded motoneuron activities," *Annals of biomedical engineering,* vol. 47, no. 6, pp. 1357-1368, 2019.

[16] C. Dai, Y. Zheng, and X. Hu, "Estimation of muscle force based on neural drive in a hemispheric stroke survivor," *Frontiers in neurology,* vol. 9, pp. 187, 2018.

[17] Y. Zheng, and X. Hu, "Interference removal from electromyography based on independent component analysis," *IEEE Transactions on Neural Systems and Rehabilitation Engineering,* vol. 27, no. 5, pp. 887-894, 2019.

[18] A. Hyvärinen, and E. Oja, "Independent component analysis: algorithms and applications," *Neural networks,* vol. 13, no. 4-5, pp. 411-430, 2000.

[19] Y. Zheng, G. Wang, and J. Wang, "Is using threshold-crossing method and single type of features sufficient to achieve realistic application of seizure prediction?," *Clinical EEG and neuroscience,* vol. 47, no. 4, pp. 305-316, 2016.

[20] Y. Zheng, G. Wang, K. Li, G. Bao, and J. Wang, "Epileptic seizure prediction using phase synchronization based on bivariate empirical mode decomposition," *Clinical Neurophysiology,* vol. 125, no. 6, pp. 1104-1111, 2014.

[21] X. Hu, N. L. Suresh, C. Xue, and W. Z. Rymer, "Extracting extensor digitorum communis activation patterns using high-density surface electromyography," *Frontiers in physiology,* vol. 6, pp. 279, 2015.

neural conduction in explanted peripheral nerve fibers," *Nature Communications,* vol. 9, no. 1, pp. 4403, 2018.